Since January 2020 Elsevier has created a COVID-19 resource centre with free information in English and Mandarin on the novel coronavirus COVID-19. The COVID-19 resource centre is hosted on Elsevier Connect, the company's public news and information website.

Building and Environment 160 (2019) 106197

Contents lists available at ScienceDirect

Building and Environment

journal homepage: www.elsevier.com/locate/buildenv

Displacement ventilation with radiant panel for hospital wards: Measurement and prediction of the temperature and contaminant concentration profiles

Narae Choi[a,*], Toshio Yamanaka[a], Kazunobu Sagara[b], Yoshihisa Momoi[c], Tomoya Suzuki[d]

[a] Department of Architectural Engineering, Graduate School of Engineering, Osaka University, 2-1 Yamadaoka, Suita, Osaka, Japan
[b] Shikoku Polytechnic College, 3202 Gunge-cho, Marugame, Kagawa, Japan
[c] Department of Architecture and Civil Engineering, Graduate School of Engineering, University of Fukui, 3-9-1 Bunkyo, Fukui, Japan
[d] Kobe City, 6-5-1 Kano-Cho, Chuo-Ku, Hyogo, Japan

ARTICLE INFO

Keywords:
Displacement ventilation
Radiant panel
Personal exposure
Air distribution

ABSTRACT

Displacement ventilation (DV) is known to provide high air quality and ventilation efficiency. With DV, a contaminant interface is formed in a room, and the air quality in the occupant zone below the contaminant interface height can be kept clean. This paper proposes a DV system to solve the serious odor problem in hospital wards. A vertical radiant panel that can be controlled individually is suggested as a complementary heating system. In order to study the influence of the panel on the displacement ventilated room, the temperature and contaminant concentration profiles were examined under different panel conditions: the distance between the panel and bed, height of the panel, surface temperature of the panel, and supply airflow rate. When the radiant panel was heated, it created a stronger plume than the human body, which produced contaminated air. When there was space between the radiant panel and bed, the contaminated air was locked up before reaching the ceiling. Personal exposure of a standing person was also investigated because the contaminated interface is generally lower than the breathing zone of a standing person with DV. The zonal model and improved zonal model were validated by a comparison of their results with the measured contaminant concentrations.

1. Introduction

The aging population in Japan has dramatically increased more than any other developed country. The statistics Bureau, Ministry of Internal Affairs and Communications in Japan reported that those who are 65 or over made up the 35.6 million and 28.1% of the total population in Sep. 2018. It is so far the highest proportion in the world. This has increased demand for hospital and welfare facilities for the elderly, and the indoor environment of these facilities has begun to attract considerable attention. A hospital ward is a place where inpatients live and get treated, and they spend most of their time in the infirmary. For this reason, both high indoor air quality and comfortable environment are required. Since a hospital ward is also a workplace for healthcare providers, the indoor environment for workers should also be considered.

An unpleasant odor in hospital wards is one of the most perplexing problems for indoor environments in Japan. An uncomfortable environment due to odor leads to a myriad of problems that contribute to the stress levels of patients, healthcare workers, and visitors [1]. Itakura and Mitsuda [2] surveyed nurses working in hospitals throughout the country, finding that more than 75% perceived a malodorous odor problem. Thus, the odor-related issues in hospital wards need to be addressed.

Displacement ventilation (DV) is considered to be an attractive ventilation system because of its high effectiveness and air quality [3,4]. Healthy indoor air quality is particularly important in the hospital environment, hence several studies have examined the suitability of DV to hospital wards. Since severe acute respiratory syndrome (SARS) affected the world in 2003, many studies have focused on whether DV can prevent droplet infection or not. Qian et al. [5] investigated hospital wards with three different ventilation systems: displacement, mixing, and downward ventilation. Their results showed that DV had worse efficiency in removing infectious droplets than other ventilation systems when the lying patient exhaled facing sideways. The exhaled jet from the source manikin penetrated a long distance along the exhaled direction. On the other hand, there are also other studies

* Corresponding author.
E-mail address: choi@arch.eng.osaka-u.ac.jp (N. Choi).

https://doi.org/10.1016/j.buildenv.2019.106197
Received 30 March 2019; Received in revised form 7 June 2019; Accepted 7 June 2019
Available online 08 June 2019
0360-1323/

Nomenclature

A_f	Floor area (m^2)
B_p	Width of the panel (m)
B_w	Width of the wall (m)
C	Normalized contaminant concentration (−)
C_b	Contaminant concentration at the breathing height outside the breathing zone (−)
C_e	Contaminant concentration of the exhaust air (−)
C_{exp}	Contaminant concentration of the inhaled air (−)
$C_{exp\text{-}m}$	Measured contaminant concentration of the inhaled air (−)
$C_{exp\text{-}p1}$	Predicted contaminant concentration of the inhaled air (Brohus and Nielsen model) (−)
$C_{exp\text{-}p2}$	Predicted contaminant concentration of the inhaled air (Using inhalation shares from Zhu et al. [29]) (−)
C_d	Contaminant concentration in the lower zone (−)
C_l	Contaminant concentration in the locked-up air (−)
C_f	Contaminant concentration at the floor (−)
C_m	Measured contaminant concentration at a point in the room (−)
C_p	Specific heat at the constant pressure of the air (J/kg K)
C_s	Contaminant concentration in the supply air (−)
C_{st}	Contaminant concentration at the contaminant interface (−)
C_u	Contaminant concentration in the upper zone (−)
D	Molecular diffusion coefficient of the contaminant (m^2/h)
D_t	Turbulent diffusion coefficient of the contaminant (m^2/h)
D_p	Distance between the panel and bed (m)
H_p	Height of the panel (from the floor to the bottom end of the panel) (m)
N	Number of contaminant sources (−)
M	Contaminant emission (m^3/s)
P_p	Convective heat flux of the panel (kW)
P_h	Convective heat flux of the human (kW)
T_0	Room air temperature at the height of the thermal plume generated by the lying manikin (°C)
T_p	Temperature of the panel surface (°C)
T_m	Temperature of the ambient air around the plume (°C)
T_{ac}	Room air temperature near the ceiling (°C)
T_{af}	Room air temperature near the floor (°C)
Q_s	Supply airflow rate (m^3/h)
Q_d	Downward airflow rate along the wall at the height y (m^3/h)
Q_{dr}	Downward airflow rate at the height y (m^3/h)
Q_h	Thermal plume airflow rate from the human (manikin) (m^3/h)
Q_p	Thermal plume airflow rate along the radiant panel (m^3/h)
Q_u	Upward airflow rate along the wall at the height y (m^3/h)
Q_{ur}	Upward airflow rate at the height y (m^3/h)
Δy	Vertical width of the small wall part (m)
y	Height above the floor (m)
y_d	Height of the lower edge of the contaminant interface layer (m)
y_{exp}	Height of the breathing zone (m)
y_l	Height of the contaminant stagnation (m)
y_o	Height of the thermal plume generated by the lying person (manikin) (m)
y_{st}	Height of the contaminant interface height (stratification height) (m)
y_u	Height of the upper edge of the contaminant interface layer (m)
y_{vl}	Height of the virtual heat source (m)
η	Height ratio of the interface to the contaminant interface layer
η_e	Effectiveness of entrainment in the human boundary layer
ρ	Air density for normal room temperature (kg/m^3)

which have indicated that DV is an effective ventilation system for air infection wards [6–8]. Li et al. [6] examined the exposure risk for the co-occupant under displacement, mixing and underfloor ventilation by the numerical study. As a result, it was found that DV could provide better air quality when the droplet residuals are smaller than 5 μm and the co-occupant is located a certain distance from the source. Berlanga [7] et al. demonstrated that the exhaled contaminant could go up with the plume of the source manikin successfully when the manikin that exhaled contaminant air was facing up. The suitability of DV for avoiding nosocomial infection is still controversial [9], what is clear is that DV is superior to other ventilation systems when the contaminant is emitted with positive buoyancy force or is combined to the thermal plume of a heat source. Cross-infection control is a paramount issue for ventilation systems of hospitals; however, most nosocomial diseases are communicated by direct and indirect contact rather than airborne route [10]. Furthermore, most hospitals contain a greater number of general wards compared with infection isolation wards, and unpleasant odors in general wards are now highly problematic. Unpleasant odors in the ward are diffused from human bodies or their discharges, and because the human body is also a heat source, these odors are guaranteed to go up with the plume. This paper proposes using a DV system to solve odor issues rather than controlling infections in the hospital ward.

Thermal comfort should also be considered for a comfortable indoor environment. Local discomfort due to a vertical temperature gradient is often considered as a disadvantage of DV [11]. Moreover, DV cannot be used as a heating system [12], so a complementary heating and cooling system is needed. Inpatients in hospital wards usually lie in a bed, so the vertical temperature gradient would not affect their thermal comfort. However, patients are also more susceptible to the thermal environment than healthy people, and each patient may have different levels of thermal sensitivity depending on their condition [13,14]. Since there was a restriction on the ratio of the one-patient ward, most hospital wards in Japan have more multiple beds. Hence, an individually controllable heating and cooling system is desirable. In this study, a vertical radiant panel that can be personally controlled by a patient was used as an ancillary heating system to acquire a thermally comfortable environment.

The interface layer of a displacement ventilated room exists above the occupied zone. While lying or sitting occupants inhale clean air in the lower zone of the interface layer, the breathing zone of standing occupants is occasionally located in the upper zone. Brohus and Nielsen [15] carried out full-scale measurements of personal exposure and found that standing occupants could inhale cleaner air than the contaminant concentration at the same height because they inhale air inside the boundary layer around bodies. Healthcare providers work on their feet, so it is critical to examine the personal exposure of standing occupants in wards to solve the odor problem.

For the design of an indoor air environment, it is essential to correctly predict the air temperature and contaminant concentration distribution. Previous studies have already developed several models to predict the vertical temperature profile of a displacement ventilated room [16–19]. However, there are few models for predicting the contaminant concentration distribution. The interface layer is known to be formed at the neutral height, where the supply airflow rate and air flow rate of the convective plumes are equal [20,21]. This neutral height is often considered as a flat line, although there is an intermediate stratified layer between the lower zone and the upper zone because of molecular and turbulent diffusion in actual situations. Lin et al. [22]

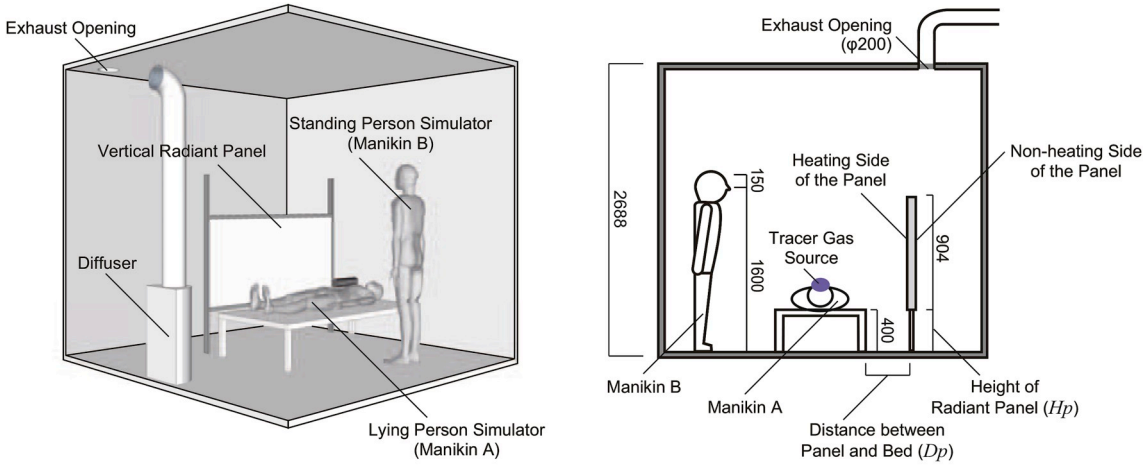

(a) Schematic view of the experimental room (b) Section view of the experimental room, [mm]

Fig. 1. Schematic and section view of the experimental room.

suggested two-layer stratification model and studied on the thickness of the intermediated stratified layer as well. Yamanaka et al. [23] developed a zonal model that considers diffusion. Suzuki et al. [24] suggested an improved zonal model to predict the contaminant concentration distribution when the contaminated air is locked up. Inagaki et al. [25] and Yamanaka et al. [26] developed a coupled zonal model that can predict the temperature and contaminant concentration profiles simultaneously.

In this study, the temperature and contaminant concentration profiles were measured in a full-scale displacement ventilated room with a vertical radiant panel. The personal exposure of standing occupants was also examined. The zonal model and improved zonal model were validated by a comparison of their calculated results with the experimental results.

2. Experiment

2.1. Experimental setup

Experiments were carried out in an environmental chamber with a length of 3000 mm, width of 3000 mm, and height of 2688 mm. The experimental arrangement is shown in Fig. 1. All envelopes (four walls, ceiling, and floor) were insulated with a 50 mm thick polystyrene layer. The surroundings of the chamber were kept at 23–26 °C throughout the experiments except for the underfloor. Fresh air was supplied from a semicircular wall-mounted diffuser (D = 400[mm], T = 260[mm], H = 750[mm]) that was located on the floor in the middle of the wall. The supply air temperature was maintained at 25 °C. The exhaust grill had 200φ holes and was on the ceiling near the wall where the diffuser was placed. Two person simulators were used: one was placed on the bed (manikin A, lying down), and the other was located between P7 and P8 (manikin B, standing). Manikin B was only used in experiments investigating the personal exposure of a standing person. The manikins were wrapped in polyvinyl chloride (PVC) heating cable at equal intervals and put in sweat suits. The heat generation from manikin A was controlled at 40 W, and the heat generation from manikin B was controlled at 75 W to represent the sensible heat load. CO_2 was used as the tracer gas to simulate the odor from the human body and was distributed from a tube on manikin A. The CO_2 flow rate was controlled at 0.5 L/min with a mass flow controller. The tube for inhalation was placed on the face of manikin B. Inhalation was assumed to be steady, and the inhaled air was maintained at 14.4 L/min to represent the average amount of one breathing cycle [27]. For the vertical radiant panel, hot water was provided from a water tank installed outside the chamber. The surface temperature of the radiant panel was monitored, and the water temperature was controlled to achieve the target surface temperature with the heater and cooler inside the water tank.

Fig. 2 shows the horizontal and vertical measurement points for the

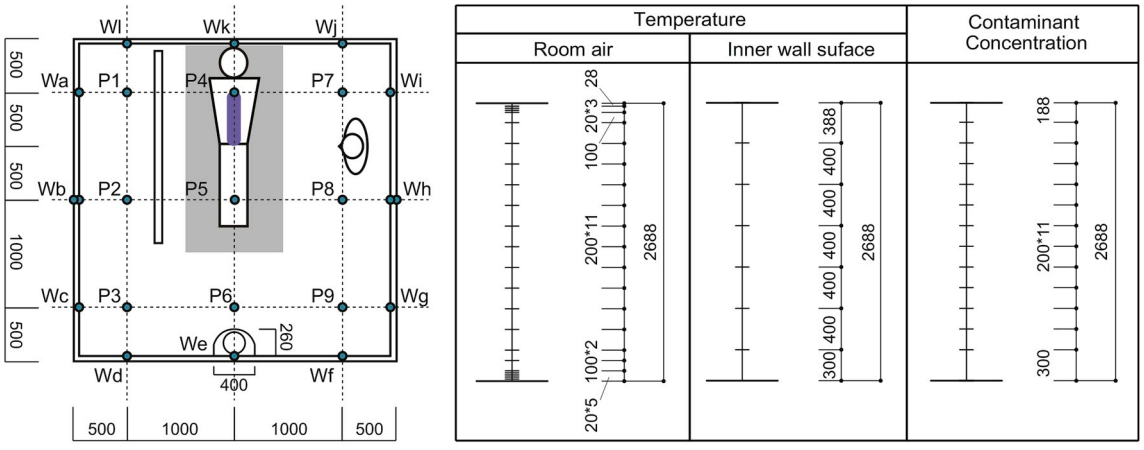

(a) Plan view of the experimental room and horizontal measurement points (b) Vertical measurement points

Fig. 2. Horizontal and vertical measurement points of the temperature and contaminant concentration.

Table 1
Experimental conditions to examine the influence of the vertical radiant panel.

Cases	Supply airflow rate Q_s [m^3/h]	Distance between the panel and bed D_p [m]	Height of the pane H_p [m]	Temperature of the panel surface T_p [°C]
Case 1	100	0	0.4	40
Case 2	200	0	0.2	40
Case 3	200	0	0.4	23
Case 4	200	0	0.4	30
Case 5	200	0	0.4	40
Case 6	200	0	0.8	40
Case 7	200	0.05	0.4	40
Case 8	200	0.1	0.4	40
Case 9	200	0.2	0.4	40
Case 10	200	0.4	0.2	40
Case 11	200	0.4	0.4	40
Case 12	200	0.4	0.8	40
Case 13	300	0	0.4	40
Case 14	300	0.4	0.4	40

temperature and CO_2 concentration. The air and wall surface temperatures were measured using T-type thermocouples (φ = 0.32 mm). There were 9 measurement points for the air temperature on the horizontal plane (P1–P9) and 22 points on the vertical line for 198 points in total. The inner wall surface temperature was measured at 12 points on the horizontal plane (Wa–Wl) and 6 points on the vertical line for a total of 72 points. The inner surface temperatures of the floor and ceiling were also measured. The external surface temperatures of each envelope were measured to calculate the heat loss through the envelopes. The contaminant concentrations were measured at 7 points on the horizontal plane (P1–P3 and P6–P9) and 12 points in the vertical direction. Non-dispersive infrared (NDIR) gas analysers were used to measure CO_2 concentration. The gas analysers were calibrated before the measurement and the reproducibility was confirmed. The measurements were performed after the temperature and concentration in the room reached a steady state.

2.2. Experimental results

2.2.1. Influence of the vertical radiant panel on temperature and contaminant concentration profiles

Table 1 presents the experimental conditions. The influences of several factors associated with the radiant panel on the temperature and concentration profile were investigated in the experiments. The following parameters were considered: distance from the panel to the bed (D_p), height of the lower end of the panel (H_p), surface temperature of the panel (T_p), and supply airflow rate (Q_s). In order to identify the positional relation between the panel and the bed, D_p and H_p were changed. Since the contaminant air was locked when D_p = 0.4 m in the pilot study, D_p was altered within the range of 0 m–0.4 m. H_p was set to 0.4 m, as high as the bed. Both H_p = 0.2 and 0.8 m were also chosen to examine when the lower end of the panel is lower or higher than the bed. The radiant panel was heated at 40 °C, which is higher than the human body temperature but not high enough to cause a danger from burns. The panel surface temperature was controlled at 23 °C for cooling and 30 °C for the neutral condition for reference. Q_s = 200 m^3/h was chosen as the standard condition because it was confirmed that the interface was formed higher than the breathing zone of lying and sitting person in the pilot study. Q_s = 100 and 300 m^3/h were adopted to carry out the measurement under the several height conditions of the contaminant interface.

In the experimental results, the horizontal axis of the vertical temperature profiles represents the temperature difference from the supply air temperature. The normalized concentration was used for the vertical concentration distribution and is defined as

$$C = \frac{C_m - C_s}{C_e - C_s} \quad (1)$$

Table 2
Experimental conditions to examine the influence of the vertical radiant panel.

Cases	Heat loss through the envelopes [W]	Heat generation of the radiant panel [W]	Heat generation of the manikin A [W]
Case 1	131	170	40
Case 2	112	173	40
Case 3	44	−23	40
Case 4	75	77	40
Case 5	97	154	40
Case 6	110	160	40
Case 7	97	158	40
Case 8	64	158	40
Case 9	63	144	40
Case 10	111	175	40
Case 11	57	147	40
Case 12	95	141	40
Case 13	99	179	40
Case 14	96	154	40

Although the temperature outside the chamber was controlled, it was still influenced by the outdoor temperature. Furthermore, it was not possible to control the underfloor air temperature. Therefore, the impact of heat loss through the envelopes slightly differed depending on the outdoor temperature in all cases. Heat loss and heat generation values of each case are presented in Table 2. The mean values of the measured inner and outer surface temperature of each wall, floor, and ceiling were used to calculate the heat loss through the envelopes. Heat generation from the panel was calculated using the differences between the inlet and outlet water temperatures.

Fig. 3 shows the influence of the horizontal distance between the panel and the bed (D_p). As shown in Fig. 3(a), temperature stratification formed in all cases. The temperature in the room increased with D_p. However, this is not because of D_p but because of the difference in heat loss through the envelopes of the chamber (Table 2). The vertical temperature differences and the temperature gradients were almost the same under the different D_p conditions. It indicates that D_p did not have much effect on the temperature distribution. There was no significant difference between cases in terms of the vertical concentration profile on the non-heating side of the panel. The contaminant interface height formed at the same level. On the other side, the contaminated air from manikin A was trapped in all cases on the heating side of the panel except for D_p = 0 m. When there was no space between the panel and bed, the plumes from the manikin A and panel merged into one plume and were efficiently exhausted. However, the locked-up phenomenon appeared when D_p was even only 0.05 m. It indicates that, when there was no space between the two heat sources, fresh air in the lower part of the room was entrained into the plume of the panel, and the two plumes rose separately. For this reason, the weaker plume from manikin A stagnated at a lower level and was unable to rise directly to the ceiling.

Fig. 4 shows the influence of the height of the panel (H_p). As H_p increased, the temperature rose at a higher part of the room (Fig. 4(a)), and the concentration interface height formed at a higher level (Fig. 4(b), (c), (e), (f)). When H_p = 0.8 m, the contaminated air was locked on the heating side of the panel, even when D_p = 0 m (Fig. 4(c)). Because the height of the bed was 0.4 m, there was space between the

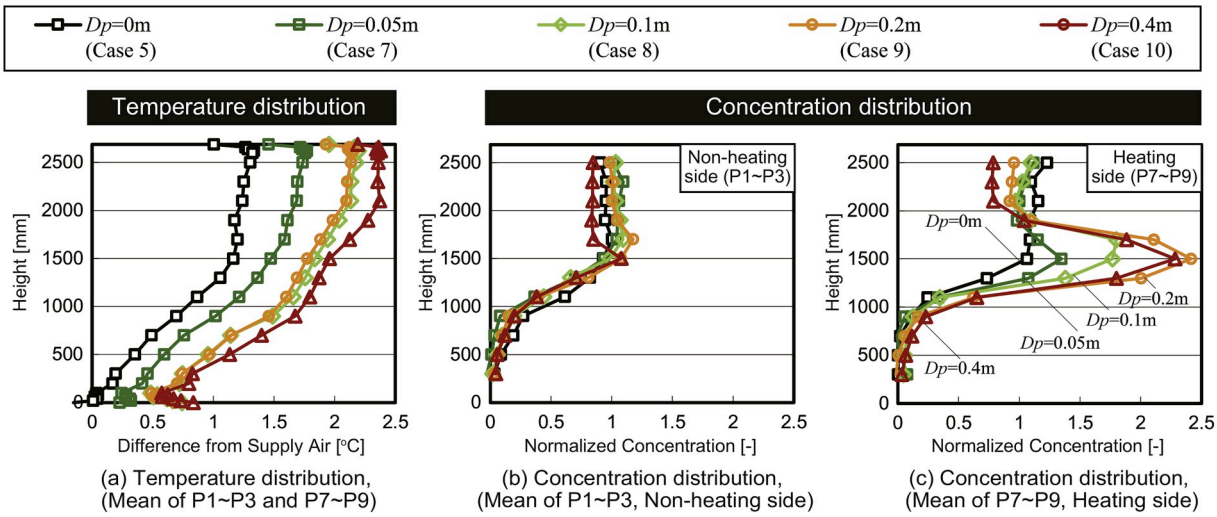

Fig. 3. Measured temperature and concentration profiles (D_p: distance between the panel and bed).

panel and bed in the vertical direction when the panel height was 0.8 m. The fresh air in the lower part was entrained through the space and went up to the ceiling without combining to the plume from the manikin A.

Fig. 5 presents the influence of the surface temperature of the panel (T_p) on the room air temperature and concentration profiles. Temperature stratification was confirmed while the room temperature was lower than the supply air temperature when T_p was 23 and 30 °C (Fig. 5(a)). Although the panel surface temperature was higher than the supply air temperature, the air temperature of the lower part had negative values in case of T_p = 30 °C. The heat loss was relatively large compared to heat generation in this case (Table 2, Case 4). The room air temperature must have been higher than the supply air if the room was completely insulated. As T_p increased, the heat load in the room became larger. This caused the vertical temperature gradient to increase. When T_p = 30 and 40 °C, the concentration in the lower part of the room was

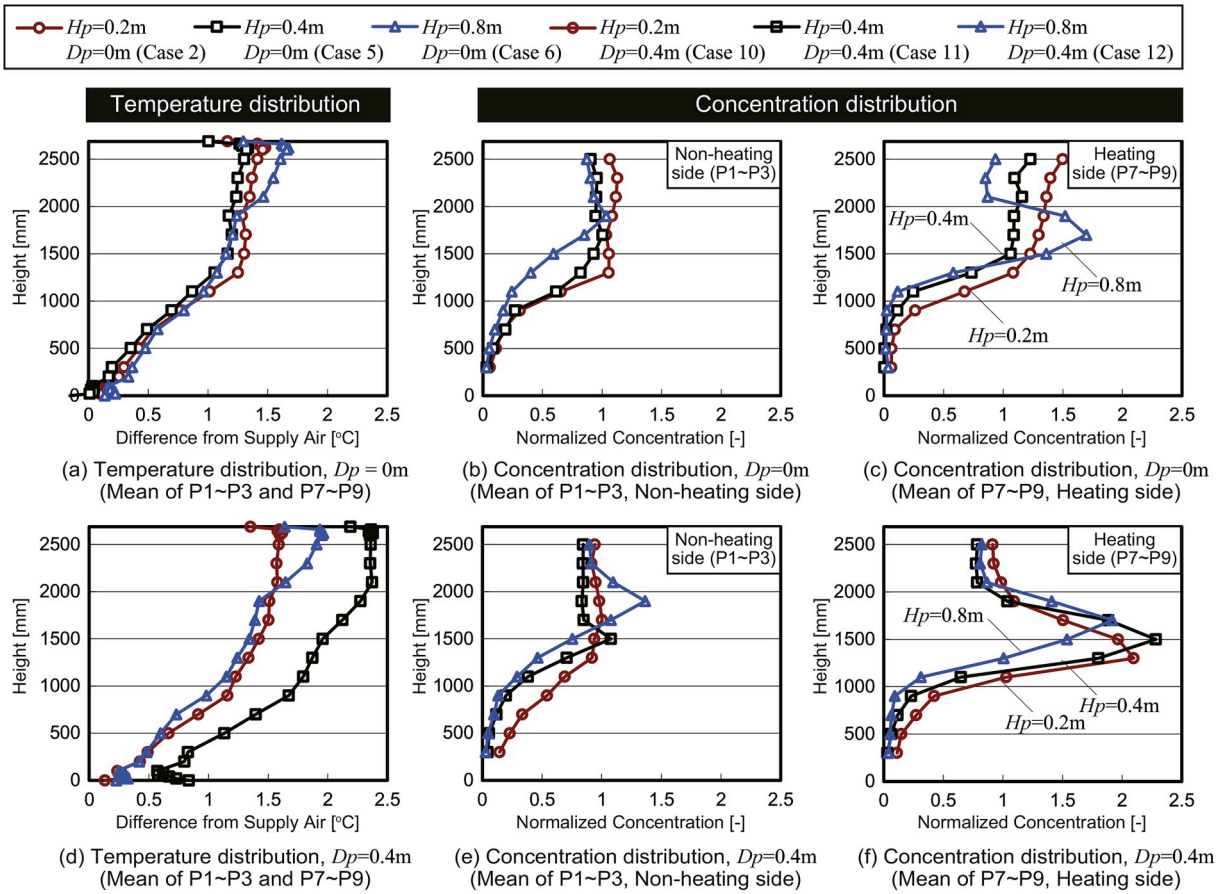

Fig. 4. Measured temperature and concentration profiles (H_p: height of the panel).

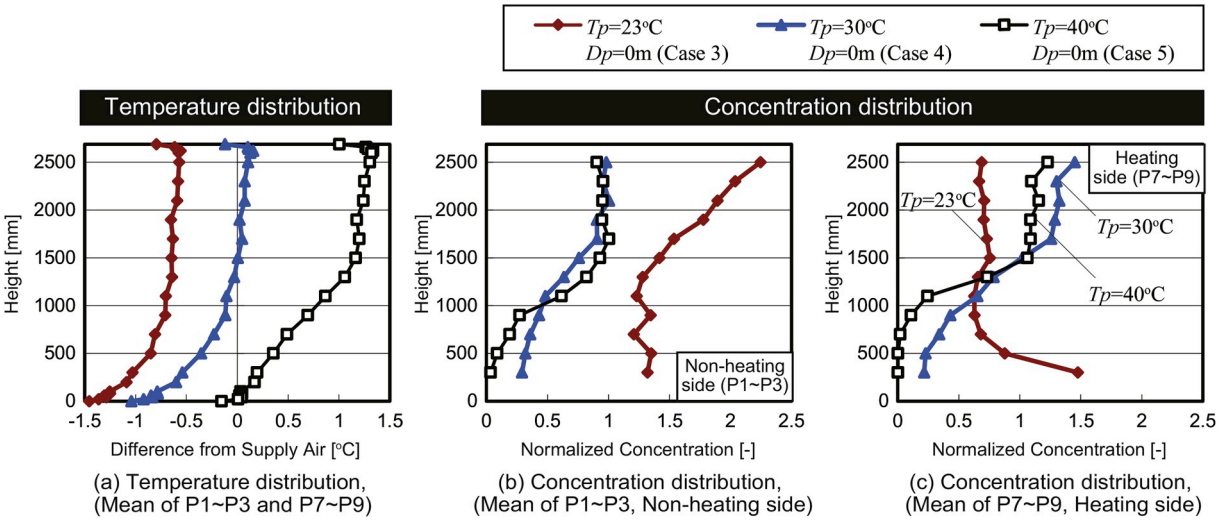

Fig. 5. Measured temperature and concentration profiles (T_p: temperature of the panel surface).

fresher than the upper part. However, when the surface temperature of the panel was lower than the supply air temperature (T_p = 23 °C), the contaminated air from the manikin A was considered to be transported from the upper part back to the lower part by the downward flow of the panel. In this case, the contaminant concentration profile was unlike general DV.

The influence of the supply airflow rate (Q_s) is presented in Fig. 6. As Q_s increased, the vertical temperature gradient became smaller and temperature stratification became weaker (Fig. 6(a), (d)). When D_p = 0 m, the contaminant concentration interface was apparent in all cases, and the height of the interface formed higher as Q_s increased (Fig. 6(b), (e)). However, when the contaminated air was trapped, no

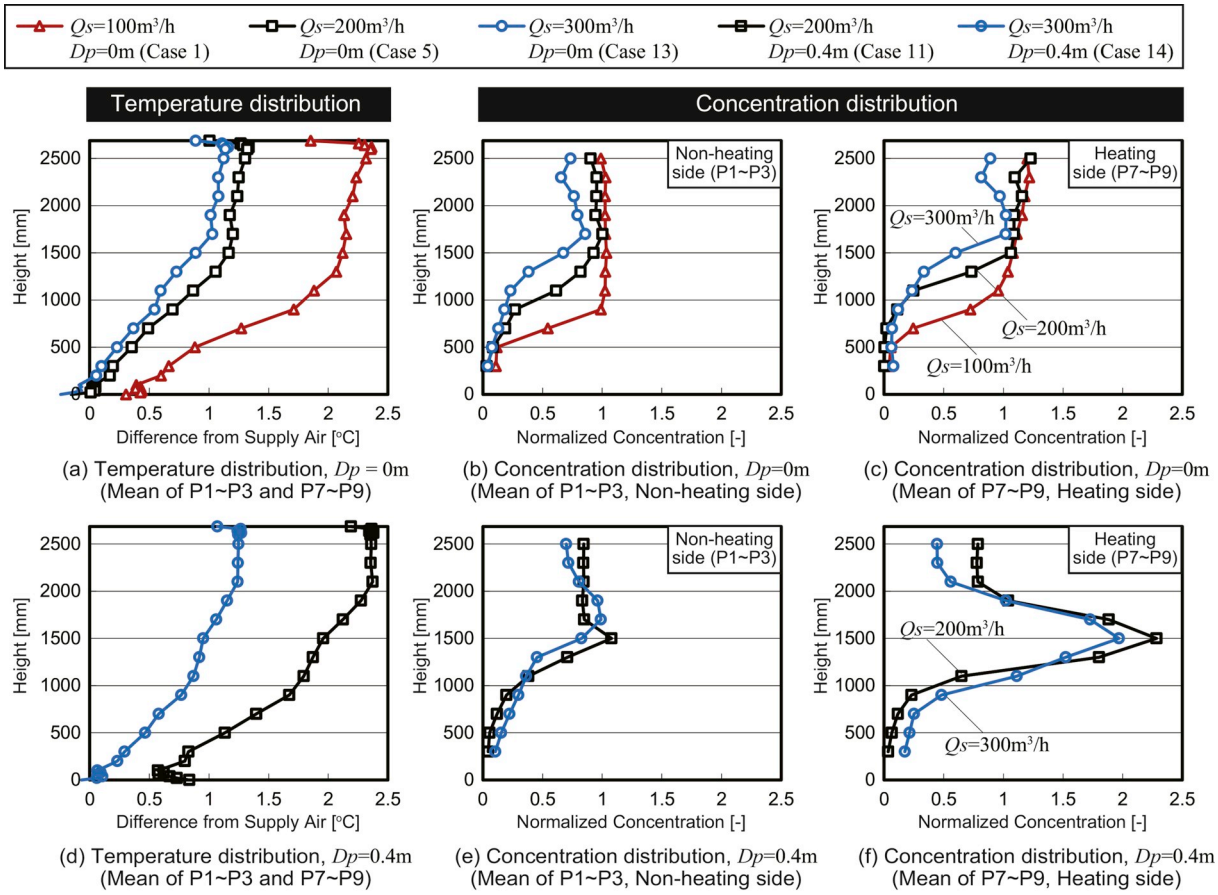

Fig. 6. Measured temperature and concentration profiles (Q_s: supply airflow rate).

(a) Case 5 (Q_s: 200m^3/h, D_p: 0m, H_p: 0.4m) (b) Case 10 (Q_s: 200m^3/h, D_p: 0.4m, H_p: 0.4m)

Fig. 7. Visualization of the contaminant plume from the lying manikin A.

Table 3
Experimental conditions of personal exposure.

Cases	Supply airflow rate Q_s [m^3/h]	Distance between the panel and bed D_p [m]	Height of the panel H_p [m]	Temperature of the panel surface T_p [°C]
Case 15	100	0	0.4	40
Case 16	100	0.3	0.4	40
Case 17	100	0.3	0.4	–
Case 18	200	0	0.4	40
Case 19	200	0.3	0.4	40
Case 20	200	0.3	0.4	–
Case 21	300	0	0.4	40
Case 22	300	0.3	0.4	40
Case 23	300	0.3	0.4	–

significant difference was evident between the neutral heights of Q_s = 200 and 300 m^3/h (Fig. 6(f)).

The plume from the lying manikin A is visualized using smoke in Fig. 7. When the radiant panel and bed adjoined each other (Case 5, Fig. 7(a)), the smoke from the lying manikin A merged with the convection flow along the panel and rose to the ceiling. However, when there was space between the panel and bed, the smoke was locked-up and the clean air which was entrained into the plume of the panel from below was accumulated near the ceiling.

2.2.2. Personal exposure of standing person

In order to examine personal exposure at different neutral heights, experiments were performed with three different supply airflow rates. Two different distances between the panel and bed were set up to compare personal exposures with and without contaminant stagnation. The unheated panel condition was added to change the heat load inside the chamber. Under the unheated panel condition, the panel was placed in the experimental chamber without heating or cooling. The measurement conditions are presented in Table 3.

The measured personal exposures and concentration profiles of the surrounding air are shown in Fig. 8. The minimum and maximum values of the measured exposures are also provided. As previously known, the inhaled air concentrations were less than the air concentration at the same height because of the entrainment effect of the plume around the body. The larger supply airflow rate created the higher neutral height. The inhaled air concentration decreased as the concentration interface height increased. When the supply rate was lower, the personal exposure was close to the concentration of the surrounding air at the breathing zone height. With contaminant stagnation, personal exposure increased.

The thermal plume around a standing person should be examined in order to accurately predict the personal exposure. If the convection flow along the body is known, personal exposure can be estimated as follows:

$$C_{exp} = \frac{\int_0^{y_{exp}} Q_h'(y) C(y) dy}{Q_h(y_{exp})} \quad (2)$$

$Q_h(y)$ is the plume airflow rate around the standing person and $Q_h'(y)$ is the entrained airflow rate to the plume at height y in the above equation.

Brohus and Nielsen [15] suggested a prediction model for the personal exposure in a displacement ventilated room. They found a simple relation between the effectiveness of entrainment in the human boundary layer (η_e) and y_{st}/y_{exp} through experiments and several previous studies. Their prediction model defines the personal exposure as follows:

$$C_{exp} = C_b - \left(\frac{y_{st}}{y_{exp}}\right)(C_b - C_f) \quad (3)$$

However, the measured contaminant concentration profiles in this study indicated different properties from the experimental results of Brohus and Nielsen. The contaminant interface was not a flat line and y_{exp} was sometimes located in the contaminant interface layer. C_b was greater than the concentration of exhausted air in some cases, especially when the contaminated air was locked up. Hence, their prediction model cannot be used as is. Based on their assumption that the entrained air flow rate is equal at every height, the personal exposure is

given by

$$C_{exp-p1} = \frac{\int_0^{y_{exp}} C(y)dy}{y_{exp}} \quad (4)$$

Zhu et al. [28] studied the distribution of the inhalation region with experiments using a thermal manikin and computational fluid dynamics (CFD) analysis. Inhalation region means that the ratio of the air at any position to the total inhaled air. They measured the inhalation regions at the heights of the head, breast, waist, knee, and foot. Their results proved that the inhalation region was greater in the upper part than the lower part. They found the following instantaneous maximum shares of inhaled air from each body part [25] 100% at the head (1.5 m), 49.6% at the breast (1.25 m), 32.2% at the waist (0.95 m), and 16.3% at the knee (0.45 m). C_{exp-p2} is given as follows:

$$C_{exp-p2} = 0.5C_{head-breast} + 0.18C_{breast-waist} + 0.16C_{waist-knee} + 0.16C_{knee-foot}$$

In the present study, the inhalation shares were rounded, and the height of each body part was adjusted as follows: the head (mouth) at 1.6 m, breast at 1.3 m, waist at 1.0 m, and knee at 0.5 m. For the concentration value of each part (i.e., $C_{head-breast}$, $C_{breast-waist}$, $C_{waist-knee}$, $C_{knee-foot}$), measured contaminant concentrations between each part were averaged. For example, measured concentrations from the height of the breast to the height of the head are used for $C_{head-breast}$.

In most cases, C_{exp-p1} was smaller than the measured C_{exp-m}. When the contaminant interface was near the breathing zone height, C_{exp-p1} was close to the measured C_{exp}. C_{exp-p2} was closer to the measured personal exposure than C_{exp-p1}. When the interface formed at a lower level or the contaminant was trapped, C_{exp-p1} and C_{exp-p2} were much smaller than C_{exp-m}. For reference, the relationship between C_{exp-p1} and C_{exp-m} was examined. The linear function $C_{exp-m} = AC_{exp-p1} + B$ was used to approximate the relationship, and A = 2.154 and B = 0.075 were obtained with the coefficient of determination $R^2 = 0.85$ (Fig. 9). Although C_{exp-p1} did not match the measured result, a considerable correlation was confirmed in this study. C_{exp-m} was approximately twice as large as C_{exp-p1}.

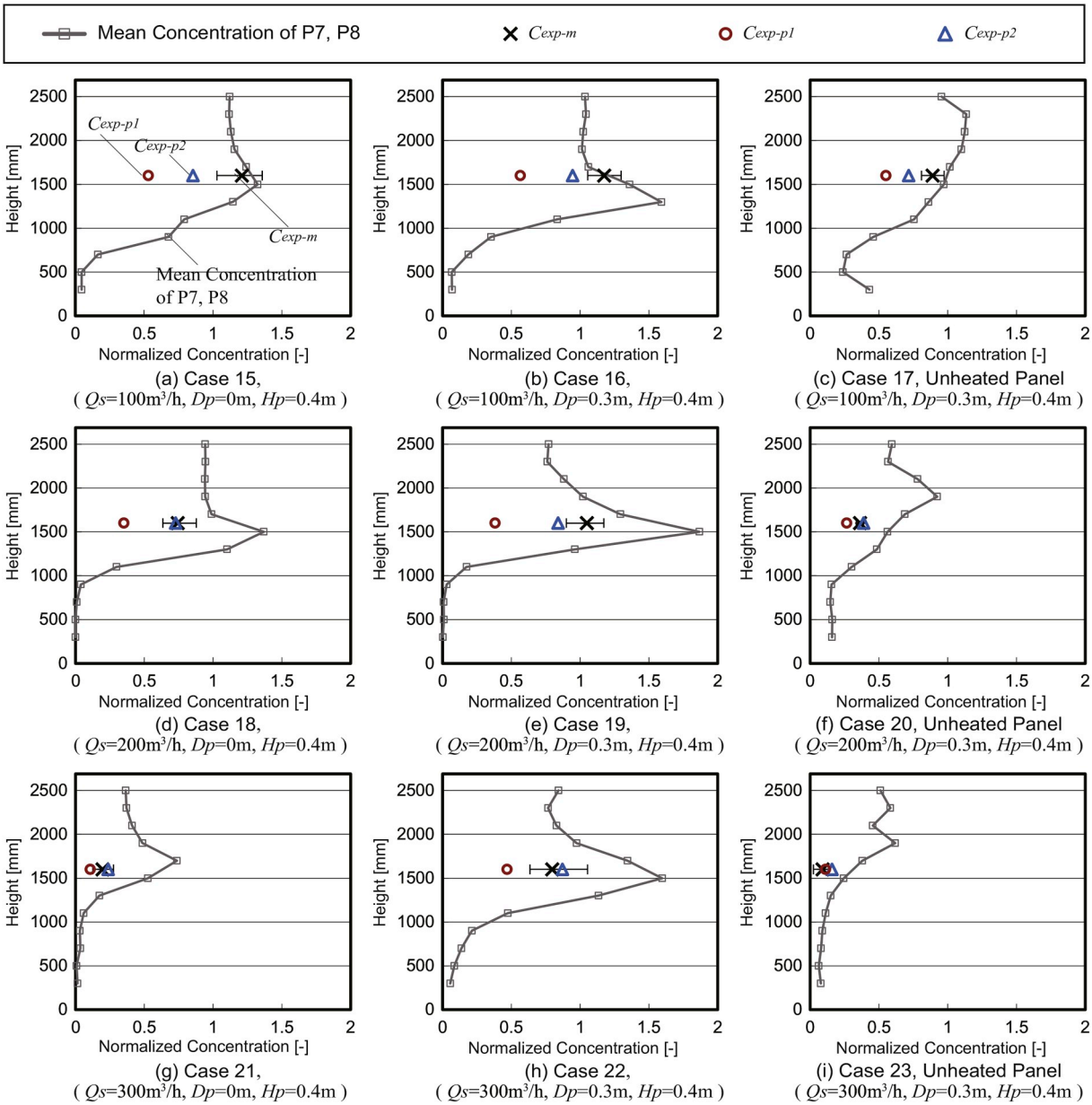

Fig. 8. Measured and predicted personal exposures of a standing person with concentration profiles. The predicted personal exposures Cexp-p1 which are calculated from measured contaminant concentrations are also shown in Fig. 8.

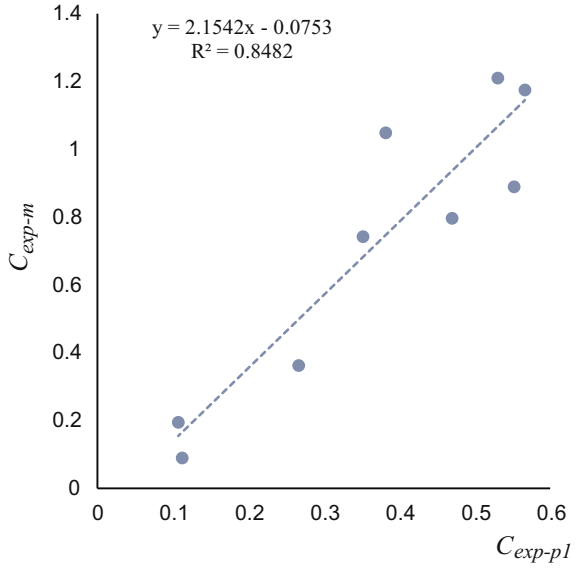

Fig. 9. The relationship between measured $C_{exp\text{-}m}$ and $C_{exp\text{-}p1}$.

The entrained air was considered to be equal at every height in the prediction model for $C_{exp\text{-}p1}$. However, the upper part of the body may entrain a larger amount of air than the lower part of the body. If $C_{exp\text{-}p1}$ is used to predict all DV situations, the freshness of the inhaled air quality could be overestimated. Another reason for the lack of accuracy in $C_{exp\text{-}p1}$ may be the difference in measurement methods. Brohus and Nielsen used a thermal manikin that could simulate actual respiration. In contrast, a simple manikin was used in this experiment, and the inhalation was regarded as steady. After all, in order to enhance the prediction accuracy, more measurements and CFD simulations are needed.

3. Calculation

3.1. Zonal model

In this study, the zonal model [23] was applied to predict the contaminant concentration profile in a displacement ventilated room. The model accounts for molecular diffusion and turbulent diffusion across the interface in order to approach the actual concentration distribution. Hence, the contaminant interface was considered to be a layer with a vertical width. The diffusion coefficient ($D + D_t$) was set to 1.8 m^2/h based on the results of a previous study [24]. The model also considers the upward and downward flows along the walls. The contaminant interface is formed at a height where the upward flow rate and supply airflow rate are equivalent:

$$Q_s = NQ_{h(y_{st})} + \sum_{k=1}^{n} Q_{uk(y_{st})} - \sum_{k=1}^{m} Q_{dk(y_{st})} \tag{5}$$

As shown in Fig. 10, the room is vertically divided into four zones. Because the incoming and outgoing contaminants are equal in each zone, the following contaminant balance equations can be obtained for zones 2–4.

Zone (2):

$$C_u Q_{dr(y_u)} = \left\{(C_u - C_d)\left(1 - \frac{\eta}{2}\right) + C_d\right\} Q_{dr(y_u)} + (D + D_t)\frac{\partial C}{\partial y} A_f \tag{6}$$

Zone (3):

$$C_d Q_{ur(y_d)} + (D + D_t)\frac{\partial C}{\partial y} A_f = \left\{(C_u - C_d)\left(\frac{1 - \eta}{2}\right) + C_d\right\} Q_{ur(y_d)} \tag{7}$$

Zone (4):

$$C_d\left(Q_{ur(y_d)} + Q_{u(y_d)} + Q_{p(y_d)} + Q_{h(y_d)}\right) =$$

$$C_u Q_{d(y_u)} + \left\{(C_u - C_d)\left(1 - \frac{\eta}{2}\right) + C_d\right\}\left(Q_{d(y_{st})} - Q_{d(y_u)}\right)$$

$$+ \left\{(C_u - C_d)\left(\frac{1 - \eta}{2}\right) + C_d\right\}\left(Q_{d(y_d)} - Q_{d(y_{st})}\right) \tag{8}$$

For the whole room, the contaminant balance can be expressed by

$$C_u = C_e = \frac{NM}{Q_s} \tag{9}$$

If all convection flow rates can be calculated, C_u, C_d, y_u and y_d are obtained by solving Eqs. (6)–(9).

A human body lying down on the bed is regarded as a horizontal linear heat source. According to previous research [24], the length of the linear source was set to 0.5 m and it was assumed to be located 0.8 m below the real location. The convection flow rate from a lying body is given by

$$Q_h = 82.43y + 24.72 \tag{10}$$

The convection flow rate along the walls is given by Ref. [30].

$$Q_w = 9.9\,|\Delta T|^{0.4} y^{1.2} B_w \tag{11}$$

However, the temperature difference between the wall surface and room air fluctuates with height. The following differentiated equation is used to forecast the air flow rate [23]:

$$\Delta Q_u(y) = \Delta Q_d(y) = 11.88\,|\Delta T|^{\frac{2}{5}} y^{\frac{1}{5}} B_w \Delta y \tag{12}$$

The walls were divided into intervals of 10 cm. The measured wall surface temperature and air temperature were used for ΔT.

The radiant panel is considered to be a vertical plane surface. Thus, the air flow rate along the radiant panel is obtained by Ref. [31].

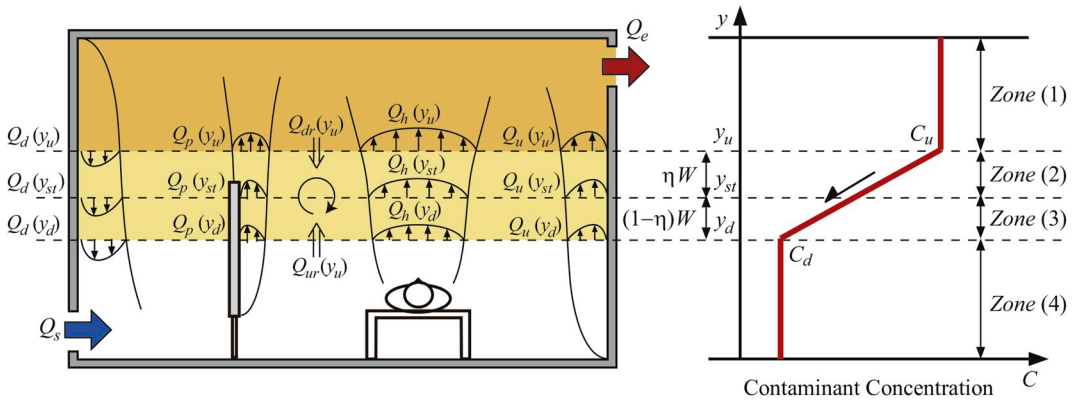

Fig. 10. Zonal model.

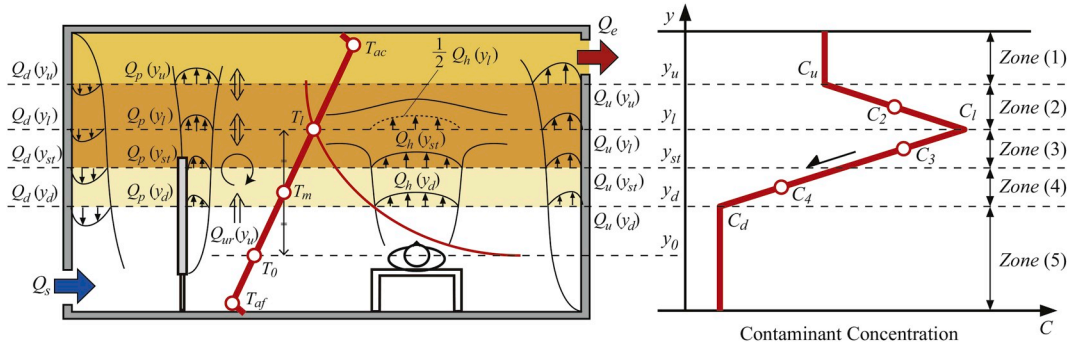

Fig. 11. Improved zonal model.

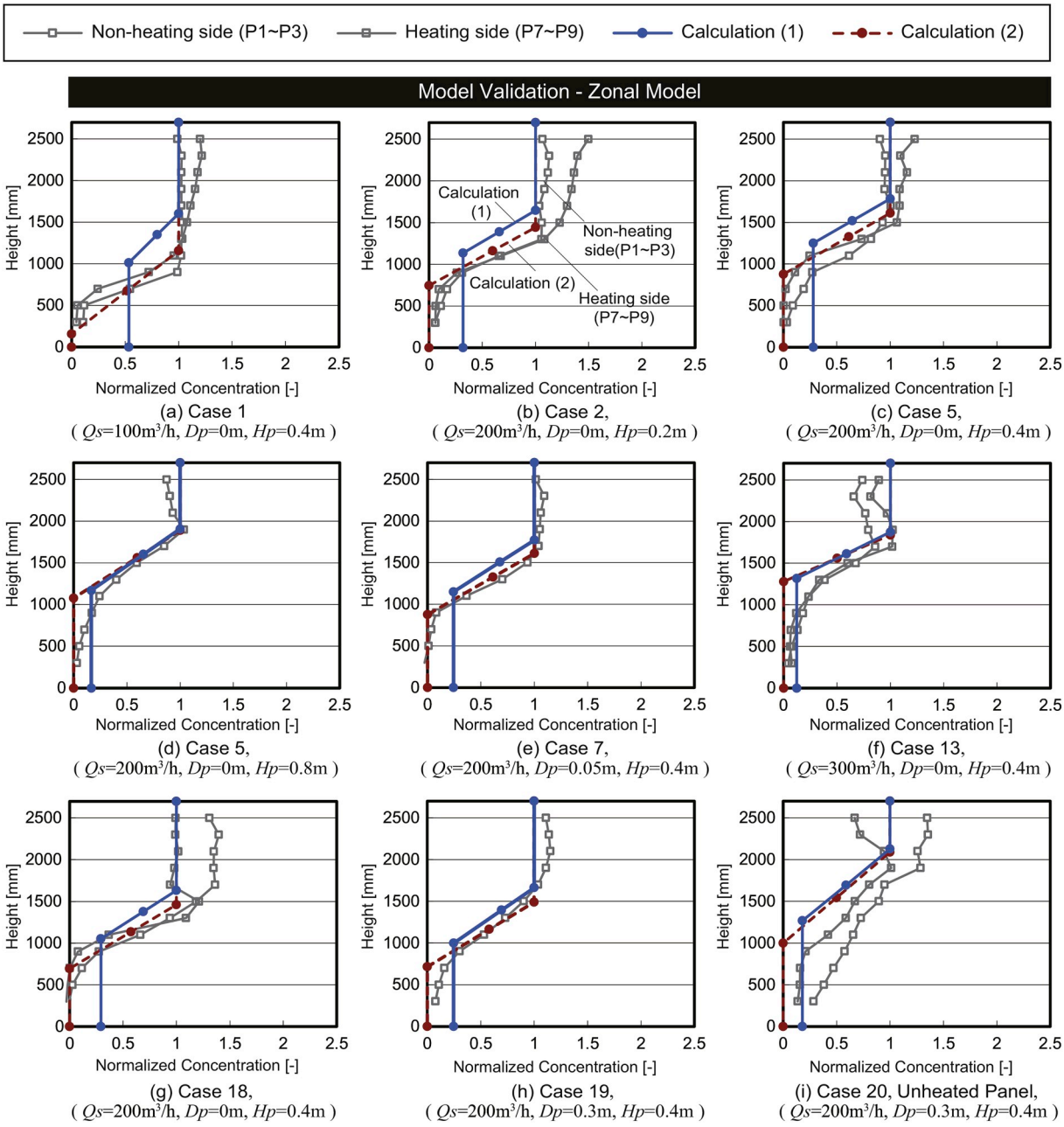

Fig. 12. Calculated results with the zonal model.

$$Q_p(y) = 79.2P_p^{\frac{1}{3.5}}(y - h_p)^{0.857}B_p \tag{13}$$

The thermal plume above the panel is estimated with the virtual source method [3]. The virtual line source is located where the airflow rates from the virtual line source and the panel would be the same at the top of the panel. The following equation is used [31]:

$$Q_p(y) = 504P_p^{\frac{1}{3}}(y + y_{vl} - h_p)B \tag{14}$$

A standing human (manikin B) is considered to be a cylinder, and Eq. (13) is applied to calculate its plume airflow rate. A virtual point heat source is used to predict the convection flow rates above the standing human body.

3.2. Improved zonal model

If a contaminated plume is weaker than plumes from other heat sources, the contaminated air cannot rise directly to the ceiling and will stagnate at the middle height in the room. Although this may not be an unusual situation for a displacement ventilated room, there have been few prediction models that have considered this phenomenon. Suzuki et al. [24] proposed the improved zonal model to predict the concentration distribution with contaminant stagnation, which is to be validated in the present study.

As shown in Fig. 11, a room is comprised of five zones. The contaminant plume is locked up at the height y_l. Half of the contaminated air is assumed to go into zone 2, and the other half is assumed to go into zone 3. The contaminant balance equation for each zone is given below.

Zone (2):

$$C_u Q_{dr(y_u)} + \frac{1}{2}\{M + C_d Q_{h(y_d)} + C_4(Q_{h(y_{st})} - Q_{h(y_d)}) + C_3(Q_{h(y_l)} - Q_{h(y_{st})})\} = C_2 Q_{dr(y_l)} + C_2\{(Q_{p(y_u)} - Q_{p(y_l)}) + (Q_{d(y_l)} - Q_{d(y_u)}) + (Q_{u(y_u)} - Q_{u(y_l)})\} \tag{15}$$

Zone (3):

$$C_2 Q_{dr(y_l)} + \frac{1}{2}\{M + C_d Q_{h(y_d)} + C_4(Q_{h(y_{st})} - Q_{h(y_d)}) + C_3(Q_{h(y_l)} - Q_{h(y_{st})})\} = (D + D_t)\frac{\partial C}{\partial y}A_f + C_3\{(Q_{p(y_l)} - Q_{p(y_{st})}) + (Q_{d(y_{st})} - Q_{d(y_l)}) + (Q_{u(y_l)} - Q_{u(y_{st})})\} \tag{16}$$

Zone (4):

$$C_d Q_{ur(y_d)} + (D + D_t)\frac{\partial C}{\partial y}A_f = C_4\{(Q_{p(y_{st})} - Q_{p(y_d)}) + (Q_{h(y_{st})} - Q_{h(y_d)}) + (Q_{d(y_d)} - Q_{d(y_{st})}) + (Q_{u(y_{st})} - Q_{u(y_d)})\} \tag{17}$$

Zone (5):

$$C_u Q_{d(y_u)} + C_2(Q_{d(y_l)} - Q_{d(y_u)}) + C_3(Q_{d(y_{st})} - Q_{d(y_l)}) + C_4(Q_{d(y_d)} - Q_{d(y_{st})}) = C_d Q_{ur(y_d)} + C_d(Q_{p(y_d)} + Q_{h(y_d)} + Q_{u(y_d)}) \tag{18}$$

For the whole room, the contaminant balance can be expressed by

$$C_u = C_e = \frac{NM}{Q_s} \tag{19}$$

The plumes are considerably affected by temperature stratification. If the plume airflow rate is assumed to increase linearly, the average temperature of the temperature at the height where the plume is

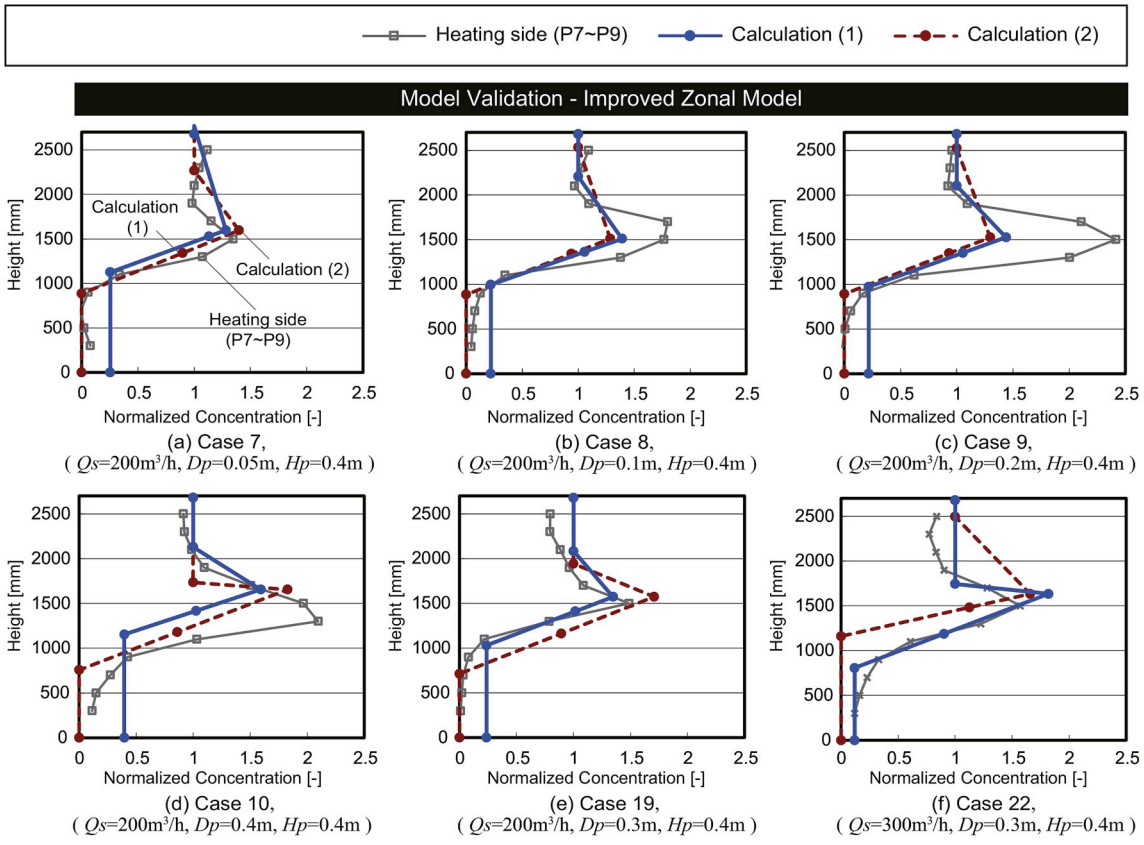

Fig. 13. Calculated results with the improved zonal model.

generated and the temperature at the height where the plume is stagnated could be used for the temperature of the entrained air. The air temperature inside the plume at height (y_l) can be expressed as follows [25]:

$$T_p(y_l) = T_m + \frac{P_h}{Q_{h(y_l)}\rho C_p} = T_{af} + \frac{\partial T}{\partial y}\cdot\left(\frac{y_l + y_0}{2} - y_{af}\right) + \frac{P_h}{Q_{h(y_l)}\rho C_p} \quad (20)$$

The plumes are locked up when there is no difference between the temperature inside the plume and the ambient temperature. Hence, the height where the plume is stagnant can be derived as follows [20]:

$$T_{af} + \frac{\partial T}{\partial y}\cdot\left(\frac{y_l + y_0}{2} - y_{af}\right) + \frac{P_h}{Q_{h(y_l)}\rho C_p} = T_{af} + \frac{\partial T}{\partial y} y_l \quad (21)$$

The measured temperature values near the floor (60 mm) and ceiling (2100 mm) were applied to get the linear temperature gradient ($\partial T/\partial y$) in this study. However, if the temperature values need to also be calculated, the temperature model could be used.

C_2, C_3, C_4, and C_{st} can be expressed as follows:

$$C_2 = \frac{C_u + C_l}{2} \quad (22)$$

$$C_3 = \frac{C_l + C_{st}}{2} \quad (23)$$

$$C_4 = \frac{C_{st} + C_d}{2} \quad (24)$$

$$C_{st} = (C_l - C_d)\left(\frac{y_{st} - y_d}{y_l - y_d}\right) + C_d \quad (25)$$

Solving Eqs. (20)–(24) yields C_u, C_l, C_d, y_u, and y_d, which can be used to obtain the predicted vertical concentration profile.

3.3. Model validation

Fig. 12 presents the calculated concentration with the zonal model and the measured results. The averaged concentration profiles on both sides of the panel (P1–P3, P7–P9) are shown for cases when the contaminated air was not trapped. In other cases, only the values of the non-heated side of the panel (P1–P3) are compared to the calculated results. The upward and downward flows along the walls were considered for calculation (1) with the above models. On the other hand, calculation (2) did not take into account convection flows on the walls.

The calculated results with the zonal model closely matched the measured contaminant profiles in most cases. When there was a considerable downward airflow in the room, the calculated height of the contaminant interface layer increased, and the contaminant concentration in the lower part also increased. In these cases, calculation (1) showed little correspondence with the measured results. One possible reason is that the measurement points of air temperature were not close enough to the walls. Calculated downward airflow rate using the measured room air temperatures and the wall surface temperatures might larger than actual situation. The downward flow was proved to affect the stratification height and contaminant concentration of the lower zone in a previous study [32]. However, the degree of effect is still unclear.

Fig. 13 shows the results of the improved zonal model with the averaged concentration distribution of the heated side of the panel (P7–P9). The calculated stagnation heights were close to the measured results. On the other hand, the concentration of the stagnation height did not correspond well with the measured results. However, whether the stagnation occurs and where it is located are more critical to predict rather than the contaminant concentration at the stagnation. As D_p gets larger, the concentration at the stagnation height becomes higher in the experiment results; nevertheless, there was no significant difference in the calculated results. When the radiant panel is close to the bed, the contaminant plume from the manikin would be entrained to the upward flow along the panel partially. If the panel is thoroughly far from the panel, two plumes would move individually. In this model, the change of the plume movement due to the distance between plumes was not reflected. Although the contaminated air was assumed to be equally divided among the upper and lower zones of the stagnation height, the actual situation may be different. The calculated stagnation height was higher than the measured results when the panel was located in the lower part (Fig. 13 (d)). The linearized temperature gradient between near the ceiling and floor was used to calculate the stagnation height. Accordingly, the calculated temperature gradient in the lower part was smaller than the actual temperature distribution, and the predicted stagnation height was higher than the measured results.

A comparison between the predicted and measured concentration is shown in Fig. 14. For zonal model, the root mean square error (RMSE) of calculation (1) is 0.25 and 0.19 for calculation (2). Even though RMSE of calculation (2) is small, it tends to overestimate the air quality

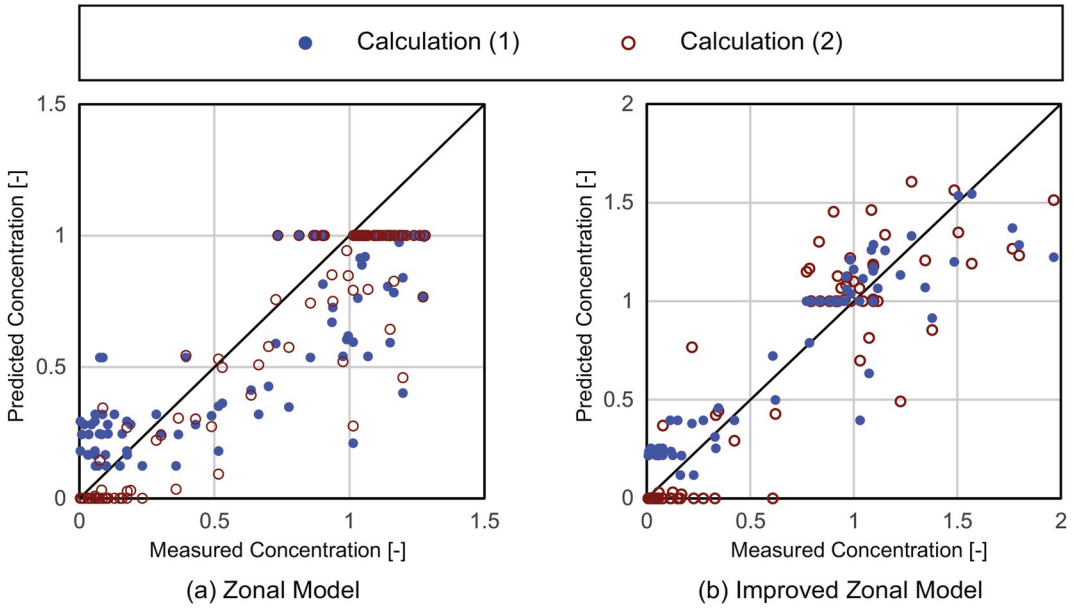

Fig. 14. Comparison of predicted and measured concentration.

(Fig. 14(a)). Calculation (1) is closer to the measured result with the improved zonal model (Fig. 14(b)). RMSE of calculation (1) and (2) are 0.22 and 0.35. The convective airflow along the wall is not considered and the contaminant concentration below the interface layer is always '0' with calculation (2). In order to avoid overrating the air freshness in the occupied zone, using calculation (1) might be better to predict the contaminant concentration profile of the room with DV.

4. Discussion

In this study, displacement ventilation (DV) is proposed to solve the unpleasant odor problem in hospital wards. Additionally, the possibility of using the vertical radiant panel as an ancillary heating or cooling system is examined.

In a room with DV, it is considered to be highly probable that DV is effective to remove the odor from the breathing zone. A lying or sitting person would not perceive the bad odor because the contaminant concentration in the lower part of the room would be nearly equal to that in fresh air. A standing person would smell the odor; however, the concentration of the odor would not be as high as it is in the ambient air due to the convective airflow layer around the body.

The vertical radiant panel should be used carefully with DV. When the vertical radiant panel is utilized as a heating system, the air in the lower part would be still clean. However, the contaminant air could be locked up in the upper part of the room if there is space between the panel and the bed. In order to remove the odor efficiently in the hospital ward, the radiant panel should be placed as close to the bed as possible. On the other hand, using a radiant panel as a cooling system is not recommended. If the surface temperature of the radiant panel is lower than the supply air, the contaminant air in the upper part would be transported to the lower part of the room, and the contaminant interface could not exist. If an additional cooling system is needed with DV, the other cooling systems, such as the floor cooling [33] and cooled ceiling [34], could be discussed.

The validity of the zonal model and the improved zonal model was proven in this paper. The contaminant concentration of the room with DV could be predicted with these models. However, the measured temperature values were used to calculate the convective airflow along the wall and the height of the contaminant stagnation in this study. The temperature profile should also be predicted in the actual design stage, so the validation using predicted temperature values is needed in further study.

5. Conclusion

Measurements were conducted to evaluate the suitability of the vertical radiant panel with DV for hospital wards. Several panel conditions were changed to investigate their influence on the temperature and contaminant concentration distribution in a displacement ventilated room. Additionally, the zonal model and improved zonal model were applied to predict the contaminant concentration profiles. The following conclusions were obtained.

- When a vertical radiant panel is utilized for heating, it generates a stronger plume than the lying manikin, which diffuses contaminated air. For this reason, the contaminated air is trapped on its way to the ceiling, and the contaminant concentration of the stagnation level is higher than the concentration of the exhaust air. In contrast, if the radiant panel is utilized as a cooling system, the downward flow along the panel descends by entrainment near the contaminated air. Hence, the contaminant concentration at the lower level is higher than general DV. These results indicate that the location of the vertical radiant panel is important when it is used as a complementary heating or cooling system with DV. When it is heated, the radiant panel and contaminant source should be placed close together. The influence of convection flow from the heat source on the contaminant concentration distribution is profound; thus, an auxiliary heating or cooling system for DV should be examined thoroughly.
- If the supply airflow rate increases, the height of the interface layer and stagnation also go up. The height of the heat source influences the temperature and contaminant distributions.
- The personal exposure of a standing person is less than the contamination of the surrounding air at the breathing zone height because the person inhales the air inside the boundary layer around the person. When the contaminated air is locked up, the concentration of the inhaled air increases. Although personal exposure would become close to the concentration of the ambient air when a person is moving, a person who stays standing up for some time could benefit from this effect. In order to predict the personal exposure more accurately, it is essential to examine the plume around the body.
- The zonal model is valid for predicting the contaminant concentration profile when there is no stagnation. The calculated results were consistent with the experimental results in all cases. However, the downward flow along the wall affects the stratification height and contaminant concentration of the occupant zone, so its influence should be further studied. On the other hand, there is good correspondence between the measured concentration profiles and calculated results with the improved zonal model. The stagnation height is accurately predicted if the temperature gradient is properly applied. The movement mechanism of the trapped air should be investigated to increase the accuracy of the improved zonal model.

Acknowledgement

The authors acknowledge the financial and technical support received from Sanki Engineering Co., Ltd. The authors are also truly grateful for the dedicated guidance and inspiration provided by Hisashi Kotani, who passed away on December 17, 2017.

References

[1] M. Horiguchi, E. Shudo, K. Sato, M. Nakamura, W. Sai, T. Ohinata, Nurse odor perception in various Japanese hospital settings, Int. J. Nurs. Sci. 2 (2015) 355–360.
[2] T. Itakura, M. Mitsuda, Research on the level of odor in a patient room of the hospital, J. Environ. Eng. 73 (625) (2008) 327–334 (in Japanese).
[3] R. Kosonen, A. Melikov, E. Mundt, P. Mustakallio, P.V. Nielsen, REHVA Guidebook No. 23: Displacement Ventilation, REHVA, Brussels, 2017.
[4] E. Mundt, Displacement ventilation systems – convection flow and temperature gradients, Build. Environ. 30 (1) (1995) 129–133.
[5] H. Qian, Y. Li, P.V. Nielsen, C.E. Hyldgaard, T.W. Wong, A.T.Y. Chwang, Dispersion of exhaled droplet nuclei in a two-bed hospital ward with three different ventilation systems, Indoor Air 16 (2006) 111–128, https://doi.org/10.1111/j.1600-0668.2005.00407.x.
[6] X. Li, J. Niu, N. Gao, Spatial distribution of human respiratory droplet residuals and exposure risk for the co-occupant under different ventilation methods, HVAC R Res. 17 (4) (2011) 432–445.
[7] F.A. Berlanga, M.R. de Adana, I. Olmedo, J.M. Villafruela, J.F. San Jose, F. Castro, Experimental evaluation of thermal comfort, ventilation performance indices and exposure to airborne contaminant in an airborne infection isolation room equipped with a displacement air distribution system, Energy Build. 158 (2018) 209–221.
[8] Y. Yi, W. Xu, J.K. Gupta, A. Guity, P. Marmion, A. Manning, B. Gulick, X. Zhang, Q. Chen, Experimental study on displacement and mixing ventilation systems for a patient ward, HVAC R Res. 15 (6) (2009) 1175–1191.
[9] Y. Li, P.V. Nielsen, M. Sandberg, Displacement ventilation in hospital environments, ASHRAE J. 53 (6) (2011) 86–88.
[10] C.B. Beggs, K.G. Kerr, C.J. Noakes, E.A. Hathway, P.A. Sleigh, The ventilation of multiple-bed hospital wards: review and analysis, Am. J. Infect. Contr. 36 (4) (2008) 250–259, https://doi.org/10.1016/j.ajic.2007.07.012.
[11] A.K. Melikov, J.B. Nielsen, Local thermal discomfort due to draft and vertical temperature difference in rooms with displacement ventilation, ASHRAE Transact. 96 (1989) 1050–1057.
[12] Q. Chen, L. Glicksman, System Performance Evaluation and Design Guidelines for Displacement Ventilation, American Society of Heating, Refrigerating and Air-Conditioning Engineers, Inc., 2003.
[13] R. Hwang, T. Lin, M. Cheng, J. Chien, Patient thermal comfort requirement for hospital environments in Taiwan, Build. Environ. 42 (2007) 2980–2987.
[14] J. Khodakarami, N. Nasrollahi, Thermal comfort in hospitals – a literature review, Renew. Sustain. Energy Rev. 16 (6) (2012) 4071–4077, https://doi.org/10.1016/j.rser.2012.03.054.
[15] H. Brohus, P.V. Nielsen, Personal exposure in displacement ventilated rooms, Indoor Air 6

(1996) 157–167.
[16] E. Mundt, The Performance of Displacement Ventilation – Experimental and Theoretical Studies, PhD Thesis, Royal Institute of Technology, Stockholm, 1996.
[17] P.V. Nielsen, Vertical temperature distribution in a room with displacement ventilation, IEA Annex 26: Energy Efficient Ventilation of Large Enclosures, IEA, Paris, 1995, p. R9509 ISSN 0902-7513.
[18] Y. Li, M. Sandberg, F. Laszlo, Vertical temperature distributions in rooms ventilated by displacement: full-scale measurement and nodal modeling, Indoor Air 2 (1992) 225–243.
[19] N.M. Mateus, G.C. da Graça, A validated three-node model for displacement ventilation, Build. Environ. 84 (2015) 50–59.
[20] M. Sandberg, C. Blomqvist, Displacement ventilation systems in office rooms, ASHRAE Transact. 95 (1989).
[21] P.V. Nielsen, Displacement Ventilation: Theory and Design, Aalborg University, Aalborg, 1993.
[22] Y.J.P. Lin, C.L. Lin, A study on flow stratification in a space using displacement ventilation, Int. J. Heat Mass Transf. 73 (2014) 67–75.
[23] T. Yamanaka, H. Kotani, M. Xu, Zonal models to predict vertical contaminant distribution in room with displacement ventilation accounting for convection flows along walls, Roomvent – 10th International Conference on Air Distribution in Rooms, FINVAC, Helsinki, 2007.
[24] T. Suzuki, K. Sagara, T. Yamanaka, H. Kotani, A. Iwamura, T. Yamashita, Prediction of vertical profile of contaminant concentration in displacement-ventilated sickroom with radiant panel, Trans. Soc. Heat. Air Cond. Sanit. Eng. Jpn. 140 (2008) 1117–1124 (in Japanese).
[25] T. Inagaki, T. Yamanaka, K. Sagara, H. Kotani, Y. Momoi, T. Yamashita, Prediction of vertical profile of temperature and contaminant concentration in sickroom with displacement ventilation (Part 2) Prediction model of vertical profile of temperature and contaminant concentration, Proceedings of the Annual Meeting of SHASE, SHASE, Tokyo, 2011, pp. 2021–2024 (in Japanese).
[26] T. Yamanaka, K. Hisashi, S. Kazunobu, Y. Momoi, T. Inagaki, M. Shinozaki, Temperature and contaminant concentration in sick room with displacement ventilation, Proceedings of the 9th International Forum and Workshop on Combined Heat, Air, Moisture and Pollutant Simulations, CHAMPS 2012), IIS, Tokyo, 2012.
[27] C.E. Hyldgård, Humans as a source of heat and air pollution, Roomvent: 4th International Conference on Air Distribution in Rooms, FINVAC, Helsinki, 1994.
[28] S. Zhu, S. Kato, S. Murakami, T. Hayashi, Study on inhalation region by means of CFD analysis and experiment, Build. Environ. 40 (2005) 1329–1336.
[29] S. Zhu, et al., Numerical analysis on pollution of inhaled air with chemical contaminant in room (Part 6) Experimental study for pathway of inhaled air around a thermal manikin with a tracer gas method, Proceedings of the Annual Meeting of the AIJ, AIJ, Tokyo, 2000, pp. 893–894 (in Japanese).
[30] E.R.G. Eckert, T.W. Jackson, Analysis of Turbulent-free Convection Boundary Layer on Flat plate, NACA Report No. 1015, NACA, Cleveland, 1951.
[31] H. Skistad, Displacement Ventilation, Research Studies Press Ltd., Baldock, 1994.
[32] M. Xu, T. Yamanaka, H. Kotani, Vertical profiles of temperature and contaminant concentration in rooms ventilated by displacement with heat loss through room envelopes, Indoor Air 11 (2001) 111–119.
[33] F. Causone, F. Baldin, B.W. Olesen, S.P. Corgnati, Floor heating and cooling combined with displacement ventilation: possibilities and limitations, Energy Build. 42 (12) (2010) 2338–2352, https://doi.org/10.1016/j.enbuild.2010.08.001.
[34] A. Novoselac, J. Srebric, A critical review on the performance and design of combined cooled ceiling and displacement ventilation systems, Energy Build. 34 (5) (2002) 497–509, https://doi.org/10.1016/S0378-7788(01)00134-7.